Journal of Marine Science and Engineering

MDPI

Article

Experimental study on motion characterization of CALM buoy hose system under water waves

Chiemela Victor Amaechi [1,2,*], Facheng Wang [3,*], Jianqiao Ye [1,*]

[1] Department of Engineering, Lancaster University, Lancaster, LA1 4YR, UK
[2] Standards Organisation of Nigeria (SON), 52 Lome Crescent, Wuse Zone 7, Abuja, 900287, Nigeria.
[3] Department of Civil Engineering, Tsinghua University, Beijing, 100084, China
* Correspondence: c.amaechi@lancaster.ac.uk or chiemelavic@gmail.com (C.V.A.), wangfacheng@tsinghua.edu.cn (F.W), j.ye2@lancaster.ac.uk (J.Y).

Abstract: The application of marine bonded hoses has increased in recent times, due to the need for more flexible conduits and flexible applications in the offshore industry. These marine structures include Catenary Anchor Leg Moorings (CALM) buoys and ocean monitoring buoys. Their attachments include floating hoses, submarine hoses and submarine cables. However, the structural performance challenges of a CALM buoy system from its hydrodynamics -water waves and other global loadings, have led to the need for this investigation. In this study, a detailed presentation on the motion characterization of CALM buoy hose system is presented. The CALM buoy is a structure with six degrees of freedom (6DoF). A well detailed experimental presentation on the CALM buoy hose model conducted in Lancaster University Wave Tank is presented using three novel techniques, which are: a digital image capturing using Imetrum systems, using Akaso 4K underwater camera, using wave gauges arranged in a unique pattern and using underwater Bluetooth sensors. The buoy model was also found to respond uniquely for each motion investigated under water waves. The results showed the higher the profile, the higher the response of the buoy. Thus, this study confirms the existence of flow patterns on the CALM buoy while floating on the water body.

Keywords: Ocean Waves; Hydrodynamics; Catenary Anchor Leg Mooring (CALM) buoy; Marine riser; Marine Hose; Motion Characterization; CALM buoy model test; Ocean engineering; Offshore Structure; Floating offshore platform (FOS).

Citation: Amaechi, C.V., Wang, F., Ye, J. Experimental study on motion characterization of CALM buoy hose system under water waves. *J. Mar. Sci. Eng.* **2022**, *10*, x. https://doi.org/10.3390/xxxxx

Academic Editor: Firstname Lastname

Received: 14 November, 2021
Accepted: date
Published: date

1. Introduction

The need for more energy resources from fossil fuels has led to the development of new floating offshore structures (FOS) for more explorations in different water depths [1-6]. These structures are induced by water waves, from shallow waters, to intermediate waters and deep waters [7-13]. This has led to the increase in the trend for the need for lighter marine structures and more flexible ones that can be easier for fluid transportation, such as marine risers [14-18]. Several innovations on FOS have been reported in ocean engineering particularly Catenary Anchor Leg Moorings (CALM) buoys [19-26]. These buoys are attached with floating hoses, submarine hoses and reeling hoses. The stability of the buoy will also determine the lifespan of the marine buoys and mooring lines. However, these marine bonded hoses are challenged with different structural issues despite being very efficient in fluid delivery [27-33].

Thus, there is the need to investigate the motion characterisation of CALM buoy systems experimentally. Currently, the design guidelines for these marine hoses are based on industry standards like API 17K, GMPHOM OCIMF 2009, DNVGL, and ABS specifications [34-39]. These hoses have some cons ranging from shorter service life, kinking, matrix cracking, damage from vessel motion, damage from hose response (snaking phenomenon and perturbations), damage from impact (line clashing), damage from disconnection (accidental operation), vibration to other structural challenges [40-44]. On the other hand, the buoys have motion responses that are relatively due to the wave loads and hydrodynamic properties on the FOS [45-50]. In real-life applications of offloading, and loading operations in offshore oil terminal systems made of single point moorings (SPM), which are made up of two main mooring configurations: Articulated Single Point Moorings (ASPM), Single Anchor Leg Moorings (SALM) and Catenary Anchor Leg Moorings (CALM) [51-55]. The SPM Buoy is a buoy that is securely anchored to the seabed by multiple mooring lines/anchors/chains, allowing liquid petroleum product cargo to be transferred. A bearing system on the buoy allows a section of it to rotate around the moored geostatic portion. The vessel will freely weather-vane all around geostatic section of the buoy while it is moored to this rotating part of the buoy with a mooring attachment. The buoy body, mooring and anchoring components, product transfer system, and ancillary elements make up the SPM system. Static legs connected to the seabed under the ocean secure the buoy body in place. The body is attached to the offloading/loading tanker by a revolving portion above the water level. The Main Bearing connects these two sections. For this same arrangement, the moored tanker will weather-vane freely around the buoy to find a secure spot. The definition of the buoy is determined by the form of bearing used and the separation of rotating and geostatic components. The buoy's size is determined by the amount of counter buoyancy needed to keep the anchor chains in place, and the anchor chains are determined by environmental factors and the size of the vessel.

Some experimental investigations have been conducted on the CALM buoy by varying the buoy skirts [56-60]. Edward & Dev [60] accessed the motion response of CALM buoy with some empirical estimation on the viscous damping. Cozijn et al. [61] conducted an experiment using a 1:20 scaled CALM buoy model, and found drag coefficient values and damping data for pitch, roll, and heave motions. These were also used to compute the coefficient of additional mass, which is 1.5 for CALM buoy hoses [61,62]. However, similar studies on buoy motion have been conducted using computational fluid dynamics (CFD) [63-65]. In principle, CFD models are developed using different discretization methods like interpolating element free Galerkin (IEFG), Boundary Element Method (BEM), and Ciarlet-Raviart mixed finite element method (FEM) and finite volume methods [66-68]. Figure 1 shows a CALM buoy maintained by Bluewater with two hawsers attached to FPSO for loading / offloading operations.

Figure 1. CALM buoy with two hawsers attached to FPSO for loading and offloading operations (Reproduced, with permission, Courtesy: Bluewater; Source: Bluewater, [69])

In this article, an experimental investigation was conducted on the motion characterization of a CALM buoy under water waves. Section 1 presents some introduction to this buoy study. Section 2 presents the experimental model of the CALM buoy, the materials and methods. Also, some assumptions on the buoy with skirt and buoy with hose model were presented. Section 3 presents the results and discussion, while the concluding remarks on the CALM buoy study are given in Section 4. The CALM buoy is a floating buoy designed to operate in six degrees of freedom (6DoFs) and is usually attached to a tanker via hawsers and a floating hose during loading operations.

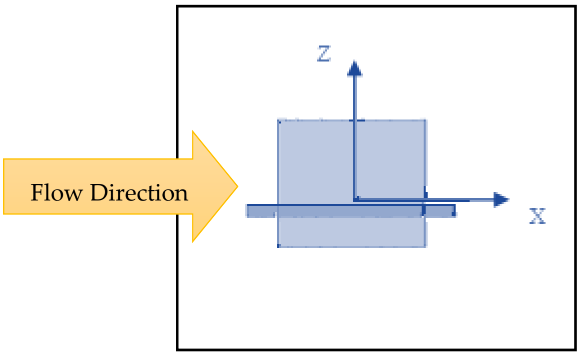

Figure 2. Illustration on the flow direction across the CALM buoy model's hull

2. Materials and Methods

The experimental modelling aspect has been presented in this section on the materials utilised in this experiment and the methodology. The materials include the buoy, submarine hoses, mooring lines and cameras, as discussed in the subsequent sub-sections.

2.1. *Experimental Setup*

For the experiment, the Lancaster University Wave Tank facility was used in all the experimental investigations. The CALM buoy test model was first tested for buoyancy, and leakage, then it was properly ballasted. It was then positioned at 5.5 m from the wave maker along the central axis of the wave tank. Figure 2 is the flow direction across the CALM buoy model's hull. The buoy model was then moored using 6 steel chain mooring lines, and 6 wave gauge were attached to the buoy skirt, as in Figures 7-10. Video recordings were also collected for each run using an underwater camera. It recorded the behavior of the hoses (submarine and floating) and the CALM buoy for different frequencies. The experimental setup showing the Lancaster University wave tank in Figure 3. The first set of the experiment was carried out using flat seabed for different frequencies. Wave gauges are attached to obtain the readings using a set-up with LabView NXG 5.1. The LabView was interfaced with a NI-DAQmx Device called National Instruments DSUB Model NI 9205. End-fittings were connected at both ends of the two hoses connected to the buoy model underneath it (submarine hoses) and one hose on the side (floating hose). Mooring lines made of 20mm-diameter steel chains were used and one end was anchored to the floor while the other end was to the skirt of the model for the CALM buoy.

Figure 3. Test basin at Lancaster University wave tank facility showing location of buoy and wave gauges used in the experiment

2.2. *Lancaster University's Wave Tank*

The experiment was conducted on Lancaster University Wave Tank as shown in Figure 10. The experimental setup was carried out on CALM buoy, as shown in Figure 3. The detailed setup for other components are presented in Sections 2.3-2.10. The dimension of the wave tank measures at 15m lengthwise, 2.5m in width and 1.7m in depth. Schematic of key features, dimensions, wave tank details, wave gauge layout, model supporting structures, and model mounting area on the wave tank is illustrated in Figure 4. The beech contains 2.5m lengthwise space leaving 12.5m lengthwise space available for use in experiments. Also, the depth is adjusted to 1.0m. The waves are generated using force-feedback control through seven (7) flappy-type paddles, designed by Edinburgh Designs, UK [70]. Each of the paddles have a capacity of producing sinusoidal waves with frequency range of 1.5 Hz to 0.5 Hz while the amplitudes as high as 100 mm. They are also capable of creating data files from both irregular and regular waves, depending on the input configuration. The wave tank facility has been used in validated studies [71-74].

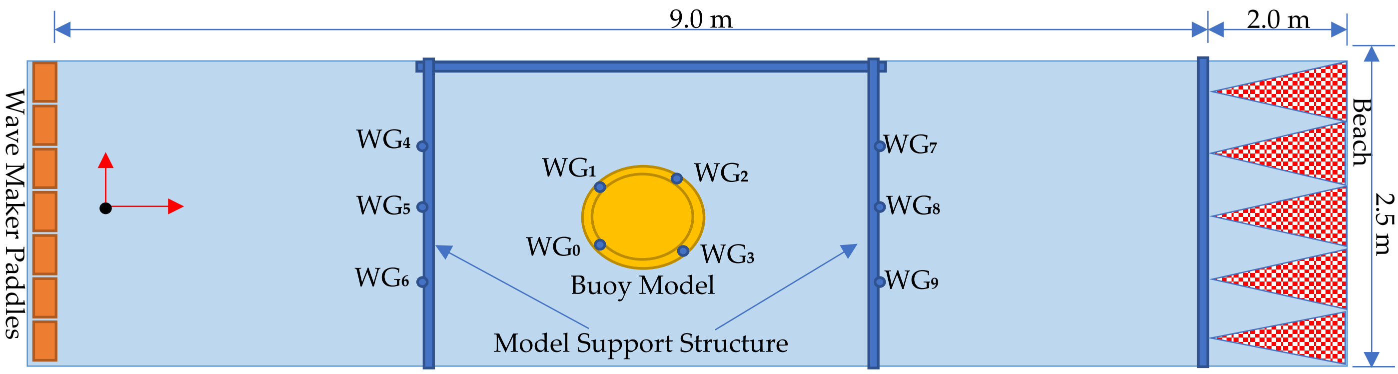

Figure 4. Schematic of key features, dimensions, wave tank details, wave gauge layout, model supporting structures, and model mounting area on Lancaster University Wave Tank

2.3. *The Buoy Model*

The buoy model is developed by considering some model assumptions including that the buoy is cylindrical, with skirt attached to it, and the skirt has thin thickness from solid plates. The fabrication of the buoy model was obtained using modelling rules. The parameters for the buoy applied in the design analysis are presented in Table 1. The model was scaled down and the model test was constructed with two submarine hoses attached underneath the buoy and one floating hose on the side, as shown in Figure 5(a-b). The results of the motion response of the CALM buoy carried out experimentally is presented in Section 3, respectively. The fabrication of the buoy model was carried out in Lancaster University Engineering Department's Mechanical Workshop. Considerations used include light metallic buoy materials, buoyancy, draft line, ballasting and scaled-modelling rules. The parameters for the buoy used in the experimental study are presented in Table 1.

Table 1. Parameters of the Model Test Buoy

Parameters	**Model Test**
Shape of buoy	Cylindrical
Depth of Water (m)	0.90
Diameter of Skirt (m)	0.68
Draft size (m)	0.15
Mass of Buoy (kg)	0.25
Buoy's Height (m)	0.20
Diameter of Buoy's body (m)	0.50

Figure 5. Images on (a) the CALM Buoy Test Model fabrication showing skirt with underneath hoses, and (b) the buoy model with floating hoses and attached wave gauges on the buoy skirt.

2.4. *Mooring Lines & Fittings*

The CALM buoy system was moored with two sections of steel chain moorings. The mooring arrangement was made up of four (4) mooring lines modelled as catenary mooring lines. The moorings are setup on the buoy and fixed via fairings attached on its skirt, as seen in Figure 6. One end of the mooring line was attached to the skirt of the cylindrical buoy while the other end was anchored to the seabed. The schematic for the setup of the model using chain moorings is presented in Figure 7. The mooring lines have the same stiffness and were 90° apart, as depicted in Figure 7.

Figure 6. Setting up the moorings on the buoy model, showing (a) the skirt with attached wave gauge fittings by mooring lines fairleads, and (b) the polyester rope and the chain mooring lines used on the moorings during the experiment

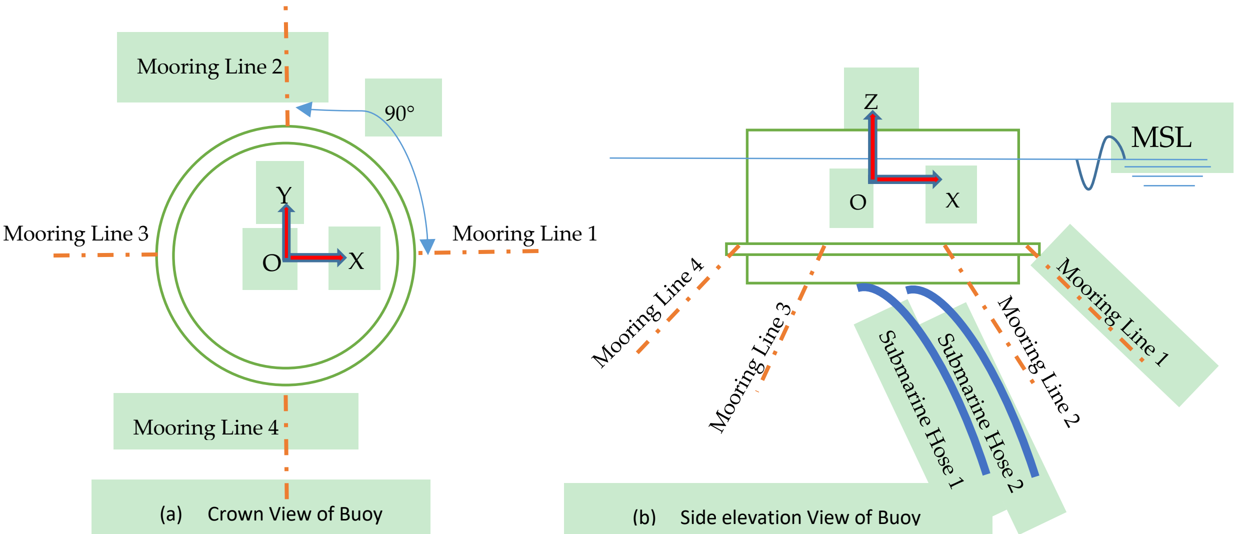

Figure 7. Arrangement of Moorings showing (a) crown view of buoy and (b) side elevation view of buoy.

2.5. *Hoses and End-Fittings*

A floating hose was also attached on the side to investigate the behaviour of floating hoses such as snaking. The hose material used in the model was about 20mm in diameter, with minimal flexible stiffness to depict an offshore hose behaviour. Four end fittings were also prepared for the hoses as shown in the Figures 6 and 8(a). As can be observed on this study, the material chosen for the floating hoses reflects real-life application [69]. These fittings are to ensure that the investigation on the hose behaviour relative to the water waves can be investigated in real time.

Figure 8. Experimental setup showing (a) floating hose attached on the buoy with the attached wave gauges on the buoy skirt, and (b) Imetrum System using DCI for Data Collection during decay test at Lancaster University Wave Tank

2.6. *Imetrum DIC (Digital Image Correlation) system*

The experiment was conducted using three different novel techniques, which are: a digital image capturing using Imetrum systems, using wave gauges arranged in a unique pattern and using underwater Bluetooth sensors. The Imetrum DIC system is shown in Figure 8(b). The study was analysed with a digital image capturing (DIC) mechanism called the Imetrum system [75,76]. This system comprises of two cameras and one non-contact system. It is designed for application in mechanical investigations, fluid and light waves-related. The Imetrum system can be used to capture both static and dynamic motions. It has been applied in capturing motion behaviour and structural investigations. Different researchers have applied the Imetrum system in obtaining results on deformation, strain, tension, compression, and displacement, as well as for other material tests [77-79]. The experiment setup details are presented in Sections 2.1-2.2.

2.7. *Wave Gauges and Readouts*

The experiment was also conducted using some wave gauges that were calibrated with crocodile clips, with the right polarity and attached to the lead ends on the model test. The maximum signal input was 5V for each of the 10 Wave Gauges (WG0, WG1, WG2, … WG9). This also aided the instrumentation as an interface to obtain the results. A network was developed in LabView [80,81] to enable the wave gauges to communicate with the readout devices and the NI DAQ sets. The wave gauges are shown in Figure 8(a), and the results obtained are presented in Section 3.

2.8. *WIT Bluetooth Gyro Underwater Motion Sensors*

Figure 9 shows two BWT901CL WIT Motion's Bluetooth gyro sensors [82] utilised in this experiment. The devices were paired to a Samsung Galaxy 8 smart phone's mini-IMU app. The Bluetooth devices had to be charged via a USB cable system before using them. The results obtained using these devices are given in Section 3. This smart phone operates on android software and the WITMotion sensor vendors provided the software download link [82,83]. The WitMotion WT901B sensor has 10 Axis AHRS IMU Sensor accelerometer, gyroscope, angle measurement, magnetometer and barometer MPU9250 that works on PC, Android and MCU, thus was suitable for use. The Samsung Galaxy 8 is a smart phone running on an Android Operating System [84,85]. The smart phone was more flexible than using the laptop PC software running on Windows Operating System. The android application called mini IMU was downloaded on the phone and on the laptop PC (personal computer) running on Microsoft Windows 10.

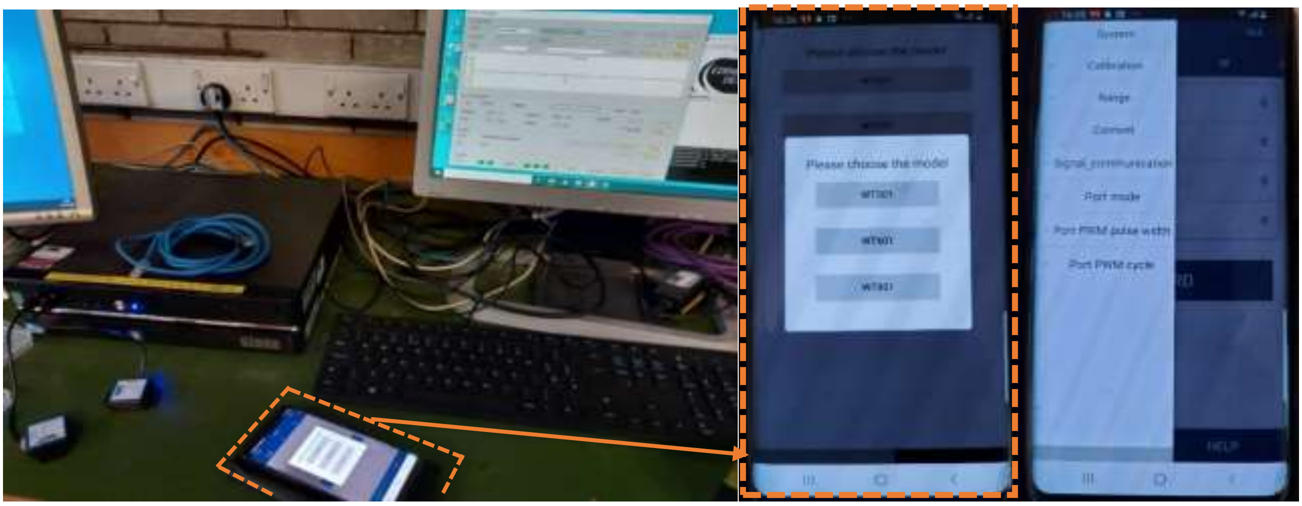

Figure 9. Experiment using 2 underwater bluetooth WIT-Motion sensors paired on Samsung Galaxy 8 smart phone, and the PC for running the wave tank calibration software

2.9. *Underwater 4K camera*

Two AKASO EK7000 waterproof-underwater cameras having Ultra High Definition (UHD) 4K image quality with 170° wide views [86], were used to record images and videos of the experimental runs. Each camera was positioned strategically to obtain the target images and video recordings for post-processing on the motion study with respect to time response. The image of the AKASO camera utilised is represented in Figure 10(a). The underwater view of the CALM buoy and submarine hoses are shown in Figure 10(b).

Figure 10. Setting up the model, showing the underwater camera, and the underwater view of CALM buoy and submarine hoses

2.10. Methodology

The experimental setup was conducted as given in Section 2.1. The methodology for the experiments were based on the phases. On this research, four different phases of the experiment were conducted. The first phase was the buoy motion study while the second was a hose response study. The third phase was a snaking hose study while the fourth is a reeling hose connection. The snaking hose study was investigated using the idealization from the marine hose developments reviewed in earlier studies [28-31].

In the experimental model presented in Figures 3-6, the floating hose was attached from a CALM buoy model to an FPSO model. It can be observed that the snaking phenomenon was evident, which is due to the water waves. Additionally, the floating hose model is of 20mm diameter and made as a flexible material to reflex the typical marine bonded hoses. It was attached to another FPSO model. Thus, this model was applied on the snaking hose study. The findings on the snaking hose study are detailed in Section 3.0. However, in the present paper, both the results of the hose snaking phenomenon and the buoy was included in Section 3. These results concentrated on the buoy motion, including the buoy attachments with hoses and the mooring lines.

2.11. Engineering Application: Numerical Studies

The engineering application of the modelling carried out numerically in previous studies using the CALM buoy model with two configurations, namely Lazy-S [87] and Chinese-lantern [88] configurations. Figure 11 shows typical numerical modelling of a CALM buoy showing two different motion positions of the buoy model in Orcaflex 11.0f. It was developed using a finite element model (FEM) in Orcina's Orcaflex, as model in Chinese-lantern configuration to confirm the engineering application as detailed in reference literature [89-92]. From these studies, the engineering application of the model was numerically conducted to reflect its applicability and some validity. Another application is a sea trial testing using S-lay configuration, published in the article [93]. In the present study, further analysis experimental studies were conducted. The recorded results were also postprocessed to confirm consistency in the CALM buoy hose motion response, as presented in Section 3. The analysis of the results from this research are based on the experimental output. However, details of by considering the hydrodynamics theory for the boundary value problem.

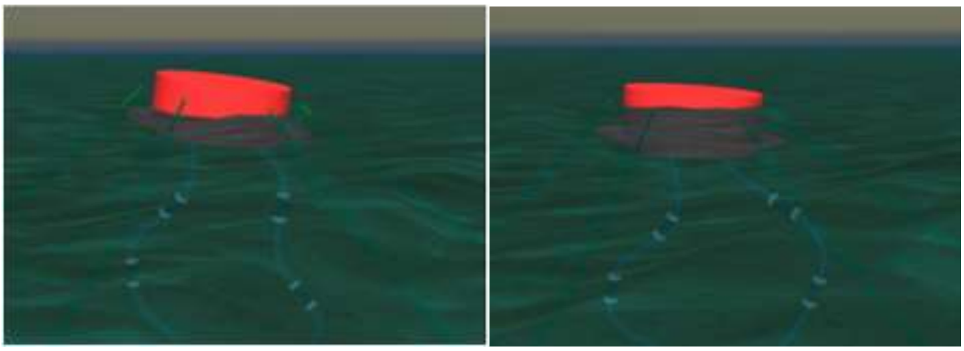

Figure 11. Numerical model of submarine hoses attached to floating buoy in Orcaflex 11.0f, showing two different motion response positions for the CALM buoy system.

2.12. *Experimental Data Postprocessing*

The experiment conducted in the wave tank was also videoed using two AKASO EK7000 Underwater Action Cameras, with 4K HD capabilities. They were positioned at two different angles, one on the side while the other camera underneath to obtain the video of the buoy and hose motions. To adequately access the motion response, some postprocessing was conducted on the recorded video output using a Tracker version 6.0.2 [94-96]. From the captured responses and results in Figures 12-13, it can be observed that for different profiles, the floating buoy has different responses captured per time.

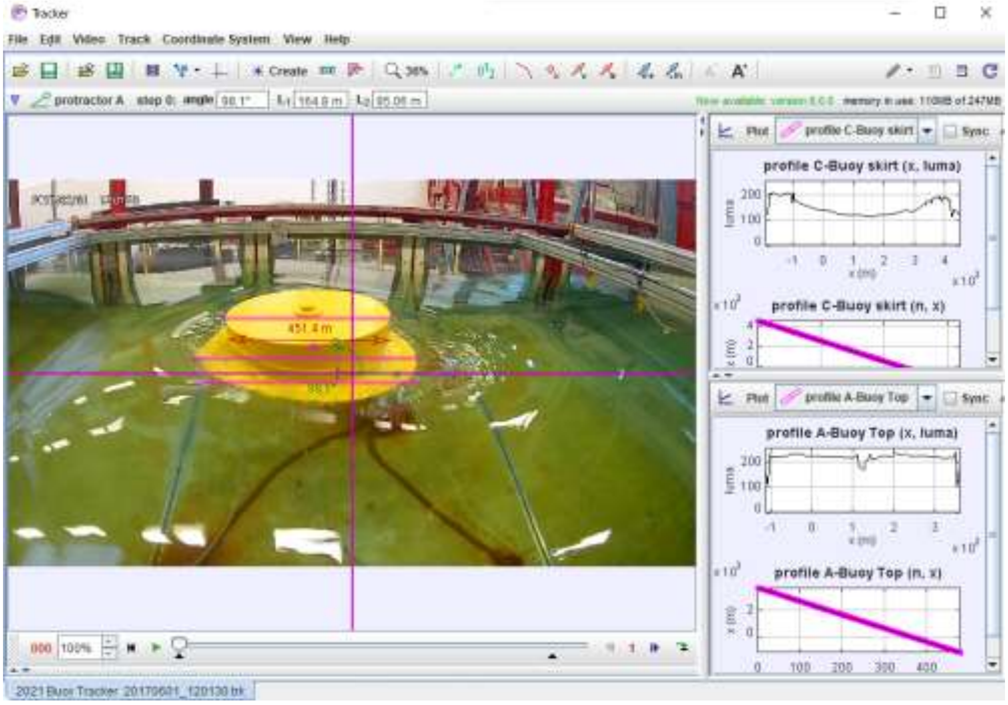

Figure 12. Result plots from the experiment on model using Tracker postprocessing software, showing profile positions.

Figure 13. Analysis from the experiment using Tracker postprocessing software for Profile A1.

3. Results and Discussion

The experimental results on the motion response of the CALM buoy with connected submarine hoses and floating hose are presented in this section.

3.1. Results from Wave Gauges and Readout

The wave parameters run on the wave tank, and the experimental model are used to obtain results on the influence of the wave angles, amplitude and frequency obtained using Wave Gauges, as shown in Figures 8. Figure 14 gives the waveform results obtained.

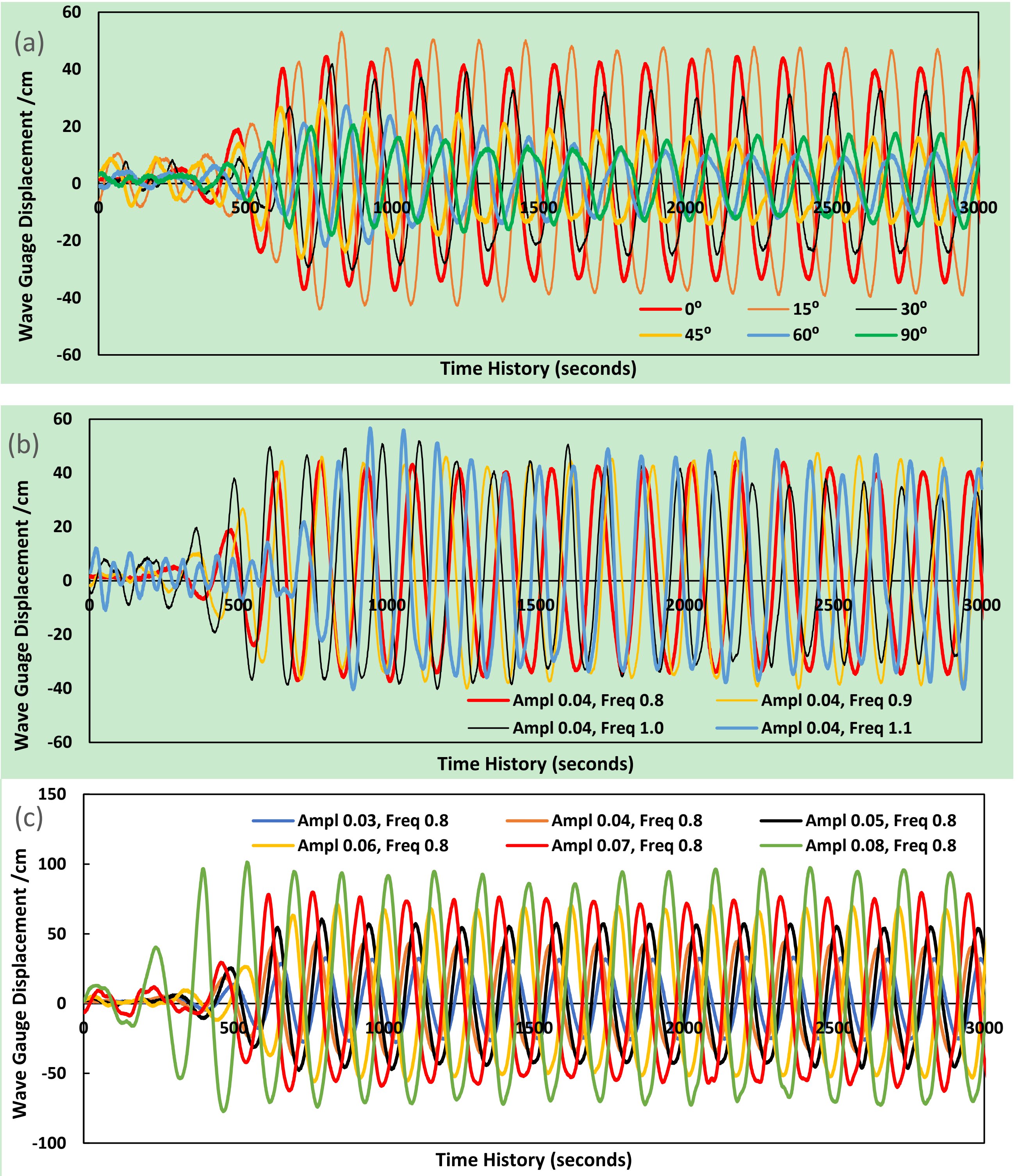

Figure 14. Results from experiment showing the effect of (a) wave angles, and (b) frequency, and (c) amplitude

From the results obtained on the wave forms in Figure 14(a), a variation in wave angles had varying amplitudes in the wave forms. The effect of frequency from the experiment as described were also conducted as presented in Figure 14(b). Using the same amplitude of 0.04m, the highest frequency was 1.1Hz, while the lowest was 0.8Hz. The effect of amplitude is seen in Figure 14(c), as the higher the amplitude, the higher the wave form.

3.2. Results from Wave Tank's Underwater Motion Sensors

The experiment was setup as described in Section 3.0 using the Bluetooth underwater sensors paired to Samsung Galaxy 8 smart phone, as shown in Figure 9. However, the phone was more flexible to use. The phone was paired to the Bluetooth device BWT901CL, and then the waves were run for the desired waves as in Tables 2 and 3. The wave parameters run on the wave tank are presented in Table 2, as obtained using the wave tank interface in Figures 3 and 9.

From Figure 15, three equations representing the profiles on: (a) wave frequency versus period, (b) surge response and (c) heave response, were obtained as follows:

$$y = 0.3339x^2 - 1.4905x + 2.1487, R^2 = 0.9986 \qquad \text{Equation (1)}$$
$$y = -0.0074x^2 + 0.0333x - 0.0208, R^2 = 0.998 \qquad \text{Equation (2)}$$
$$y = 0.0618x^2 - 0.137x + 0.077, R^2 = 0.9413 \qquad \text{Equation (3)}$$

However, further processing of the motion response against equations of motion are useful in obtaining the terms for the unknowns in each equation. Further hose motion response study can be found in literature [73,74].

In Table 2, it is noteworthy to add that these parameters were used based on the calibration on the Lancaster University Wave Tank at the wave frequency of 1Hz. The wave tank has the capacity for both tidal waves and ocean waves, however the later was utilised in this experiment. Table 3 presents the results of the experiment using a single wave direction, and the flow was calibrated for regular waves.

Table 2. Parameters for Hydrodynamic Experiment on Wave Tank

Parameters	Amplitude	Angle	Frequency	Distance	Max Runtime
Value	0.078	0.0	1.0	5.0	64.0
Unit	m	Degree (°)	Hz	m	secs

Table 3. Results of Maximum amplitude during Experimental Test

Parameters for the Wave		**Max Displacement**	
Frequency, f (Hz)	**Period, T (sec)**	**Surge (m)**	**Heave (m)**
0.5	2.0	0.01506	0.04660
0.6	1.6	0.01301	0.02640
0.7	1.4	0.01150	0.00190
0.8	1.2	0.00825	0.00240
0.9	1.1	0.00633	0.00260
1.0	1.0	0.00465	0.00220

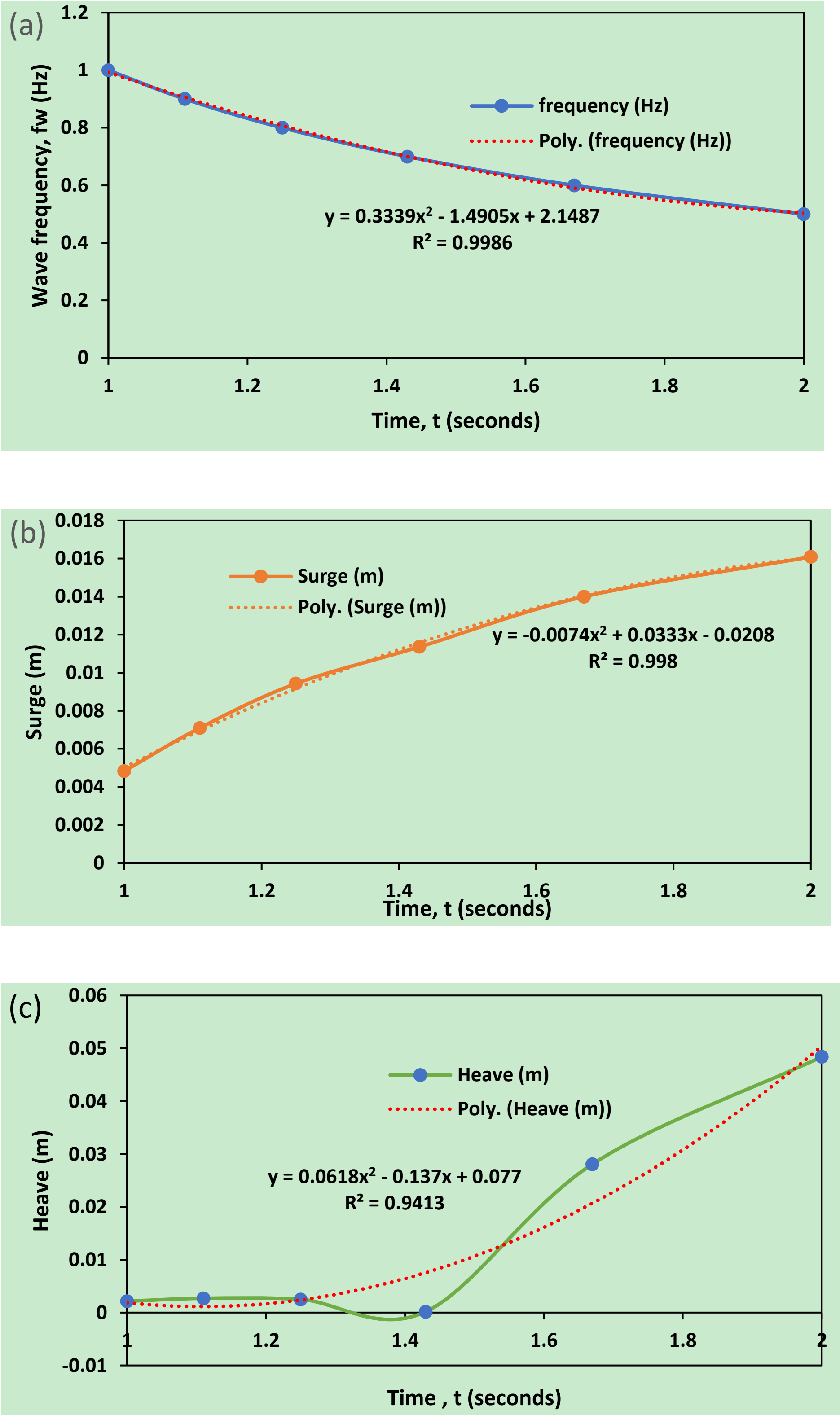

Figure 15. Result plots from the Experiment on model under maximum displaced amplitude, showing (a) wave frequency versus period, (b) surge response and (c) heave response.

3.3. *Results from DIC using Imetrum System*

The experiment was setup and also carried out as described in Section 2.0. The wave parameters run on the wave tank are presented in Table 2, as obtained using the wave tank interface in Figures 3 and 9. Table 3 presents the results of the experiment using a single wave direction, and the flow was calibrated for regular waves. The results of the experimental model were obtained in two methods: using the wave gauges via LabView and secondly via the Imetrum System for the heave and surge of the CALM buoy system. The motions in the X and Z directions were studied, as defined in Figure 2. The Imetrum system was used to perform the motion study in the section based on a method called the digital image capturing (DIC) methodology. The buoy had spots marked on it which were captured during the runup and used to obtain response against positions per time. The wave run up data in Table 3 were used to obtain the plots in Figures 16-21.

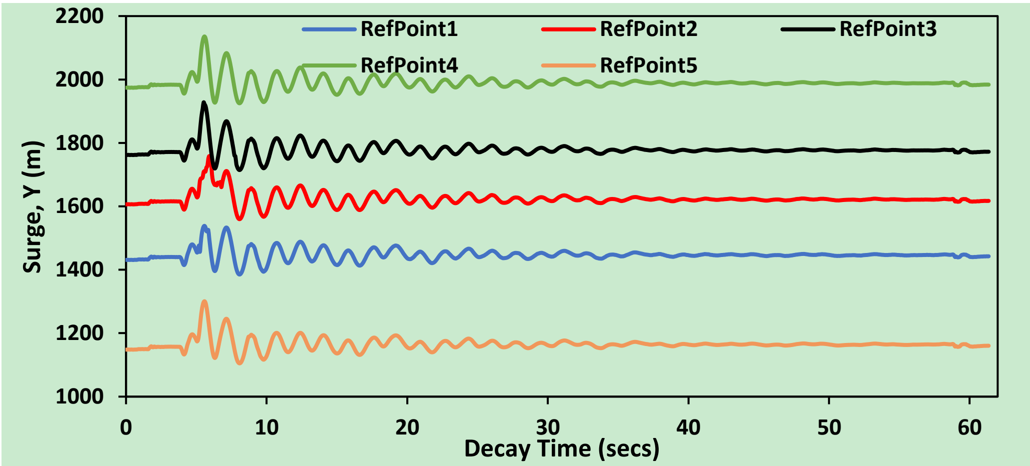

Figure 16. Surge motion for Decay Test of the CALM Buoy using the DIC with Imetrum System at 62secs run

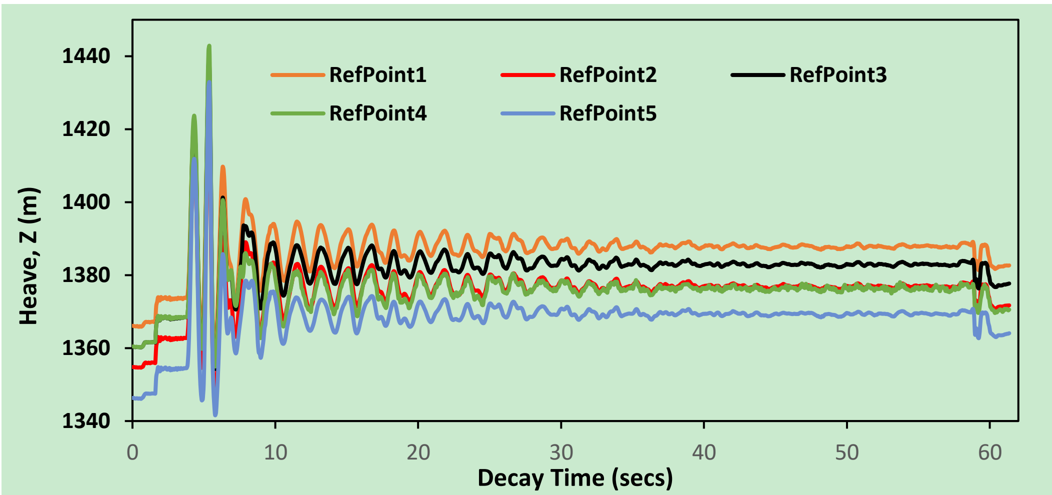

Figure 17. Heave motion for Decay Test of the CALM Buoy using the DIC with Imetrum System at 62secs run

The decay tests conducted in this section show the motion response for different motion studies conducted under three different run times of 62s and 80s. As observed in Figures 16-21, the surge response along the five (5) different reference points are consistent but show a different amplitude that is consistent, as the arrangement used was in a pattern that confirms that the results worked well as predicted and good agreement from the surge can be applied in validating similar numerical models. The first set of runs were undertaken under 62s. As recorded in the surge motion in Figure 16, the surge was highest in reference 4 at 2,117m at 5.7s. As recorded in the heave motion in Figure 17, the heave was also consistent for the five (5) reference points obtained and was also highest in reference 4 at 1,441m at 5.3s. As recorded in the roll motion in Figure 18, the heave was also consistent for the five (5) reference points obtained and was also highest in reference 4 at 2.3 degrees at 5.4s. The next set of runs were undertaken under 82s. As recorded in the surge motion in Figure 19, the heave was also consistent for the five (5) reference points obtained and was also highest in reference 4 at 2,193m at 2.7s. As recorded in the heave motion in Figure 20, the heave was also consistent for the five (5) reference points obtained and was also highest in reference 1 at 1,511m at 2.2s. Lastly, the heave motion in Figure 20 showed that the heave was consistent for the 5 reference points obtained and was also highest in reference 2 at 1.5 degrees at 2.3s. Also, this confirms the buoy response characteristics, as considered during the normal test run and the decay tests. The plots show consistency with the lines of best fit, and the equations on these relationships. On the roll motion given in Figure 21, the five (5) reference points obtained showed closed correlation for the responses. It can be observed that the response amplitude from the wave on the CALM buoy hoses are consistent. The motion video data from the experimental study was further post-processed as presented in Section 3.4.

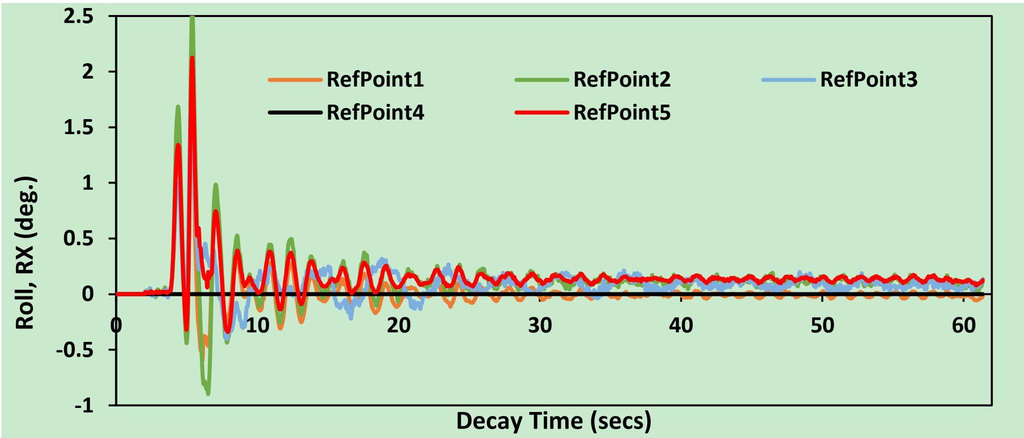

Figure 18. Roll motion for Decay Test of the CALM Buoy using the DIC with Imetrum System at 62secs run

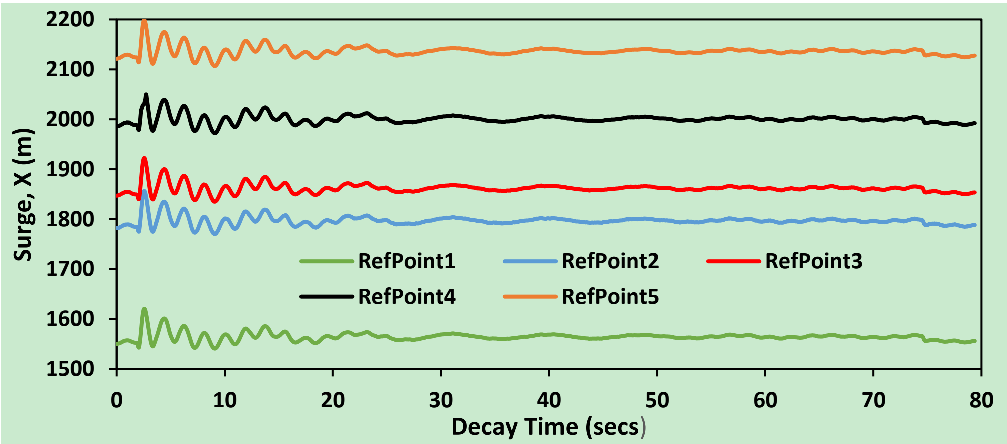

Figure 19. Surge motion for Decay Test of the CALM Buoy using the DIC with Imetrum System at 80secs run

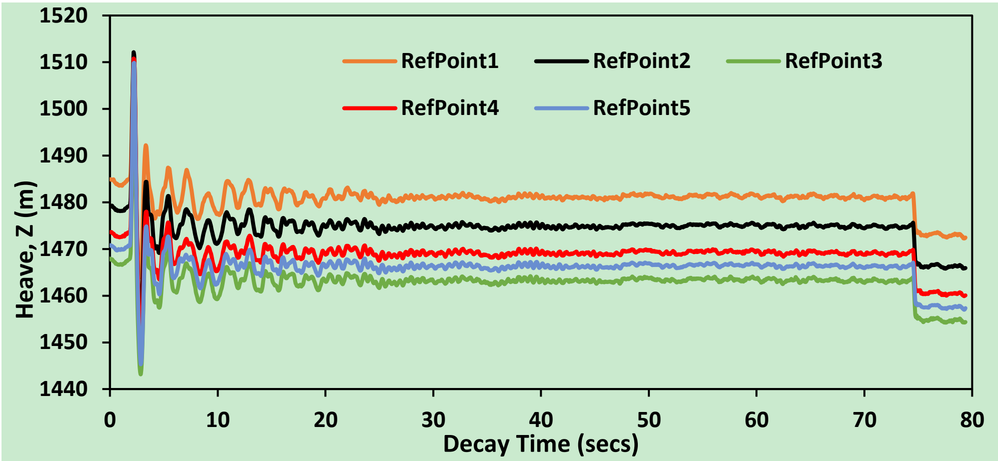

Figure 20. Heave motion for Decay Test of the CALM Buoy using the DIC with Imetrum System at 80secs run

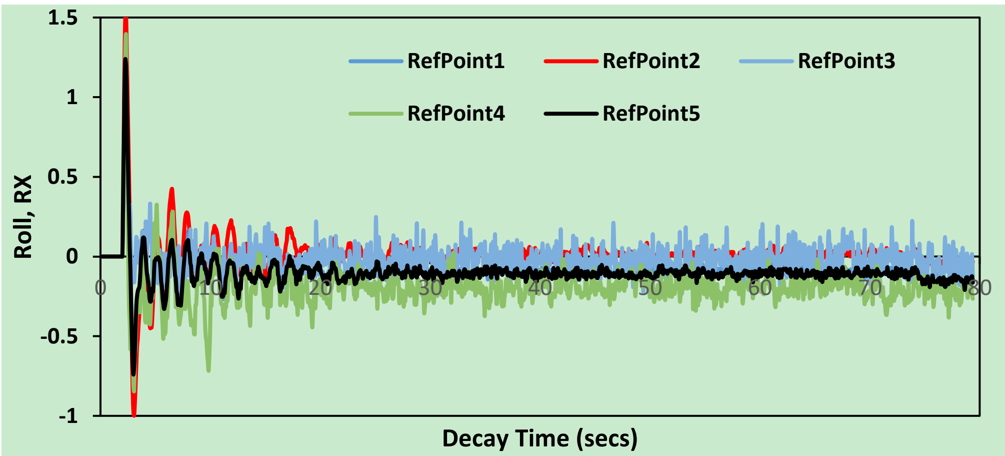

Figure 21. Roll motion for Decay Test of the CALM Buoy using the DIC with Imetrum System at 80secs run

3.4. *Results from Tracker Postprocessing*

The recorded video from this experimental study was postprocessed as detailed in Section 2.12. The postprocessing on the recorded output was conducted via the Tracker version 6.0.2. From the captured responses and results in Figures 22-23, it can be observed that for different profiles, the floating buoy has different responses captured per time. Tables 4 and 5 present result profiles for Profiles A and B respectively. It shows that the luna axis increases as the base-line axis, x decreases. This shows a decay rate of the motion response as in Section 3.3. It was observed that the profiles have different sinusoidal plots on the wave response. Figures 22-23 gives the result plots from the experiment on the buoy model under maximum displaced amplitude. In the results in Figure 22, the wave response to the four selected profiles A, A1, B, and C are presented. It shows that each profile has a different motion response relative to the selected position of the profile, based on coordinate positions. Additionally, the result of the post-processing in Figure 22 shows sinusoidal plots with least trough seen as a drop within the range of 1.1m-1.4m, implying that the motion response is time-dependent for a free-floating buoy. From the plot in Figure 23, it can be noticed that the rotation per time for each frame increases for the same angle, using 1.57°. This confirms the motion behaviour of the buoy under water waves.

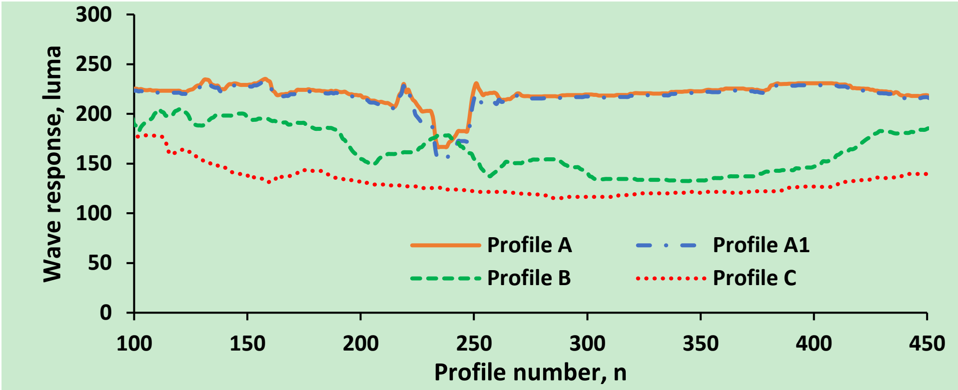

Figure 22. Result plots from the experiment for Profiles A, A1, B and C.

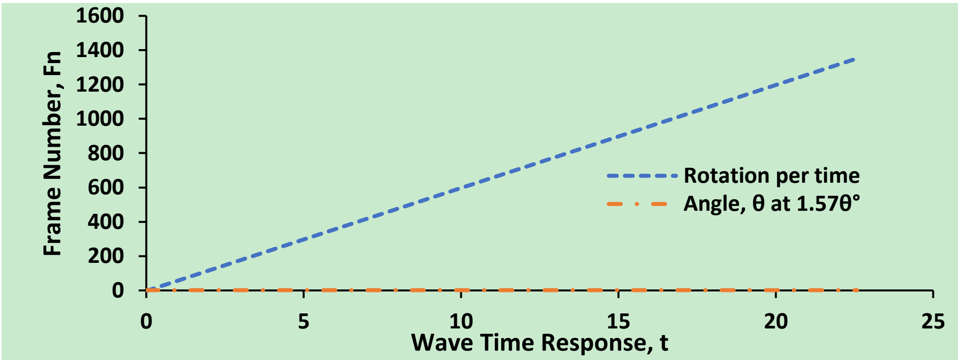

Figure 23. Plot from the experiment per frame increment for the same angle using 1.57°.

Table 4 Data Analysis from the experiment using Tracker postprocessing software for Profile A.

Horizontal, n	*Vertical, x*	*Vertical, luna*
0	363.5	172.9
1	362.5	173.9
2	361.5	170.0
3	360.5	171.0
4	359.5	149.4
5	358.5	128.4
6	357.5	121.8
7	356.5	126.8
8	355.5	117.2
9	354.5	102.2
10	353.5	125.5
11	352.5	162.5
12	351.5	238.9
13	350.5	235.4
14	349.5	227.4
15	348.5	224.6
16	347.5	218.3
17	346.5	215.5
18	345.5	213.7
19	344.5	215.1
20	343.5	215.5
21	342.5	215.6
22	341.5	212.8

Table 5 Data Analysis from the experiment using Tracker postprocessing software for Profile B.

Horizontal, n	*Vertical, x*	*Vertical, luna*
0	441.5	239.2
1	440.5	250.3
2	439.5	250.0
3	438.5	245.2
4	437.5	238.6
5	436.5	235.6
6	435.5	227.6
7	434.5	220.6
8	433.5	214.6
9	432.5	212.6
10	431.5	206.4
11	430.5	203.4
12	429.5	201.4
13	428.5	199.4
14	427.5	199.6
15	426.5	199.6
16	425.5	192.5
17	424.5	188.5
18	423.5	180.4
19	422.5	180.4
20	421.5	175.6
21	420.5	179.6
22	419.5	184.9

3.5. Discussion

The motion characteristics of a CALM buoy hull structure have been studied experimentally. Figure 13 gives the result plots from the experiment on the buoy model under maximum displaced amplitude, showing (a) wave frequency versus period, (b) surge response and (c) heave response. Decay tests were also conducted in Section 3.3. It shows motion response for different motions conducted under three different run times of 62s and 80s. From the results presented in Figures 16-21, it can be observed that the motion behaviour of the CALM buoy hose system was recorded from the experiment. In the results in Figure 22, the wave response to the four selected profiles A, A1, B, and C are presented. It was observed that the profiles have different sinusoidal plots on the wave response. However, further study on the research is recommended to look at two forms of motion analysis: vortex induced motion, which is caused by resonance from reciprocating shed vortexes, and wave induced motion, which is caused by the dynamism of wave characteristics. The wave-current interactions and wave-induced motion have been conducted experimentally. In this research, the motions caused by hydrodynamic loads were studied at the wave tank facility of Lancaster University. Since the buoy has a smaller reciprocating amplitude than larger floating structures like semisubmersibles, it can be assumed that it has a better vortex-induced motion (VIM) response. This could be due to a number of factors, including the geometric features of the buoy's diameter, the geometric shape, and the skirt positioning, and mooring configuration. Under regular waves, the wave produced motions showed a modest response, and the heave motion was found to be inversely proportional to the draught size. It is crucial to note that the results obtained from the Lancaster University wave tank facility were used for the experiment. This study results could be used in validation purposes in further studies. It can be observed in the results in this section that the buoy motion changes behaviour, relative to the water waves on both the buoy and the hoses.

The motion video data from the experimental study was further post-processed. This motion postprocessing shows that the responses are consistent on different profiles for the hydrodynamic phenomenon, particularly from the high surge response. For the results from Section 3.4, it can be observed that surge and heave motions increased as the time increased. Also, this confirms the buoy response characteristics, as considered during the normal test run and the decay tests. The plots show consistency with the lines of best fit, and the equations on these relationships. From the post-processing results using the Tracker software, some tables were generated used to make plots on the profile response per time. It shows a stable behaviour of the floating buoy under the time investigated. This study can be further developed by using some comprehensive formulations of the buoy for more understanding on the stability and dynamics behaviour of floating buoys.

4. Concluding Remarks

In this research, an experimental study on the motion characterization of a CALM buoy under water waves to investigated. Some background on the experimental model for the CALM buoy system were presented in Section 2. However, special attention is given to the CALM buoy and the skirt. The results show the peculiar characteristics, which should be considered in the design due to the drag and damping implications on it. The result of the experiment was presented on motion characterisation study. Some discussion were included on the engineering application of the system with numerical computations in earlier studies. This study is relevant to enable engineers to appropriately design CALM buoy systems, using parametric information on hose behaviour, buoy motion, buoy geometry, oceanic data and other environmental conditions.

The model highlights include the following: firstly, an experimental framework is presented on motion characterization for CALM buoy model. Secondly, a well detailed experimental presentation on the CALM buoy hose model conducted in Lancaster University Wave Tank facility. Thirdly, three different novel techniques were presented, which are: a digital image capturing using Imetrum systems, using wave gauges arranged in a unique pattern, using AKASO underwater 4K UHD action camera and using WIT-Motion underwater Bluetooth sensors. Fourthly, an experimental study on the motion scenario from the motion response study on wave angles and wave amplitudes from the CALM buoy hoses. Lastly, prediction of the CALM buoy's motion characteristics was presented from the study from post-processing using Tracker software.

The study presented response profiles based on the experimental predictions. From an offshore mechanical point of view, the motion characterisation phenomenon has been confirmed to exist as a result of response from the water waves and other global loads on the CALM buoy. The study shows more dimension on the CALM buoy in a water body and buoy motion on the marine hose. The study also showed the forces acting on the submarine hoses using diffraction theory and bending theory. Thus, will assist in both manufacturing and installation of marine hoses. The buoy model was also found to respond uniquely for each motion investigated under water waves. The results showed the higher the profile, the higher the response of the buoy. Thus, this study confirms the existence of flow patterns on the CALM buoy while floating on the water body. Further recommended is recommended for the engineering application using the Orcaflex FEM, which could be validated using experimental studies like the present study. Other studies that can be studied include the numerical fluid study or vortex flow effect on the buoy using CFD.

Author Contributions: Conceptualization, C.V.A., J.Y.; methodology, C.V.A., F.W., J.Y.; software, C.V.A., J.Y; validation, C.V.A., F.W., J.Y..; formal analysis, C.V.A., J.Y; investigation, C.V.A., F.W., J.Y.; resources, C.V.; data curation, C.V.A.; writing—original draft preparation, C.V.A.; writing—review and editing, C.V.A., F.W., J.Y.; visualization, C.V.A.; supervision, C.V.A., F.W., J.Y.; project administration, C.V., J.Y.; funding acquisition, C.V., J.Y. The author has read, confirmed and agreed to the submitted version of the manuscript to be considered for publication.

Funding: The Department of Engineering, Lancaster University, UK and EPSRC Doctoral Training Centre (DTC) are highly appreciated. In addition, the funding of Overseas Postgraduate Scholarship by the Niger Delta Development Commission (NDDC), Nigeria is also appreciated, as well as the support of Standards Organisation of Nigeria (SON), F.C.T Abuja, Nigeria. The research reported in this paper is part of the Project 51922064 supported by the National Natural science Foundation of China (NSFC), China. The article processing charges (APC) was funded by Author 1- C.V.A., with support from MDPI's JMSE.

Institutional Review Board Statement: Not applicable.

Informed Consent Statement: Not applicable.

Supplementary Materials: None provided at this time.

Data Availability Statement: The raw/processed data required to reproduce these findings cannot be shared at this time, as the data also forms part of an ongoing study.

Conflicts of Interest: The authors declare no conflict of interest. The funders had no role in the design of the study; in the collection, analyses, or interpretation of data; in the writing of the manuscript, or in the decision to publish the results.

Acknowledgments: The authors acknowledge the technical support from Lancaster University Engineering Department staff. The authors acknowledge the technical support of Mark Salisbury, Andy Baker and Nick Renninson for the support on the experiments done on the CALM buoy model fabrication. The authors recognise the support from Dr Simon Doyle of Lancaster University UK for technical support during the experimental investigation of the model and the project contributions of Dr Stephen Quayle of Lancaster University who contributed to the development of the model test are all acknowledged. The authors also acknowledge Richard Leeuwenburgh, of Bluewater for permission to use Figure 1. The authors also acknowledge the feedback given on this submission by Prof. George Aggidis of Lancaster University UK and Prof. Long-Yuan Li of Plymouth University UK. The authors are posthumously grateful to late Jeevan Mahadev Rao of Lancaster University who assisted on the experimental investigation of this project but unfortunately passed away during the COVID-19 pandemic after some health challenges. The authors also appreciate the editors of JMSE journal and the anonymous reviewers for their feedback on this submission which has helped to improve the quality of this manuscript.

Abbreviations

θ	Angle to the horizontal axis
3D	Three Dimensional
6DoF	Six Degrees of Freedom
ABS	American Bureau of Shipping
BEM	Boundary Element Method
CALM	Catenary Anchor Leg Mooring
CB	Cylindrical Buoy
CCS	Cartesian Coordinate System
CFD	Computational Fluid Dynamics
CMS	Conventional Mooring Systems
DIC	Digital Image Correlation
DNVGL	Det Norkse Veritas & Germanischer Lloyd
FEM	Finite Element Model
FOS	Floating Offshore Structure
FPSO	Floating Production Storage and Offloading
FSO	Floating Storage and Offloading
GMPHOM	Guide to Manufacturing and Purchasing Hoses for Offshore Moorings
ID	Inner Diameter
IEFG	Interpolating Element Free Galerkin

MSL	Mean Sea Level
OCIMF	Oil Companies International Marine Forum
OD	Outer Diameter
RAO	Response Amplitude Operator
SPM	Single Point Mooring
UHD	Ultra High Definition
VIM	Vortex-Induced Motion

References

1. Islam A.B.M.S., Jameel M., Jumaat M.Z., Shirazi S.M., Salman F.A. (2012). Review of offshore energy in Malaysia and floating Spar platform for sustainable exploration. Renewable and Sustainable Energy Reviews Volume 16, Issue 8, October 2012, Pages 6268-6284. https://doi.org/10.1016/j.rser.2012.07.012
2. Sadeghi K. (2007). An Overview of Design, Analysis, Construction and Installation of Offshore Petroleum Platforms Suitable for Cyprus Oil/Gas Fields. *GAU J. Soc. & Appl. Sci., 2(4), 1-16, 2007*. Available at: https://cemtelecoms.iqpc.co.uk/media/6514/786.pdf. (Accessed on 6th January, 2022).
3. Amaechi, C.V., Ye J. (2022). A review of state-of-the-art and meta-science analysis on composite risers for deep seas. *Ocean Eng.* 2021, under review.
4. Odijie, A.C., Wang, F. & Ye, J., 2017. A review of floating semisubmersible hull systems: Column stabilized unit. *Ocean Engineering*, 144 (October 2016), pp.191–202. Available at: https://doi.org/10.1016/j.oceaneng.2017.08.020.
5. Yu L.C., King L.S., Hoon A.T.C., & Yean P.C.C. (2015). A Review Study of Oil and Gas Facilities for Fixed and Floating Offshore Platforms. *Research Journal of Applied Sciences, Engineering and Technology* 6:672-679. http://dx.doi.org/10.19026/rjaset.10.2476
6. Hirdaris S.E., Bai W., Dessi D., Ergind A., Gu X., Hermundstad O.A., Huijsmans R., Iijima K., Nielsen U.D., Parunov J., Fonseca N., Papanikolaou A., Argyriadis K., Incecik A. (2014). Loads for use in the design of ships and offshore structures. Ocean Engineering 78:131-174. DOI: 10.1016/j.oceaneng.2013.09.012.
7. Sorensen, R.M., 2006. *Basic Coastal Engineering* 3rd ed., New York, USA: Springer.
8. Sorensen, R.M., 1993. *Basic Wave Mechanics: For Coastal and Ocean Engineers*, John Wiley and Sons.
9. Amaechi, C.V., Wang F., Odijie, A.C. & Ye, J., (2022). Numerical investigation on mooring line configurations of a Paired Column Semisubmersible for its global performance in deep water condition. *Ocean. Eng.* 2022, https://doi.org/10.1016/j.oceaneng.2022.110572.
10. Boccotti P. (2000). Chapter 11 Analysis Of The Wave Forces On Offshore Structures. In: *Wave Mechanics for Ocean Engineering*, 1st Edition, Elsevier Oceanography Series, Volume 64, Pages 361-392. Elsevier Science Publishers, London, UK. https://doi.org/10.1016/S0422-9894(00)80037-9
11. Boccotti P. (2015). *Wave Mechanics and Wave Loads on Marine Structures.* 1st Edition. Elsevier Science Publishers, Imprint of Butterworth-Heinemann Inc., Woburn, U.S.A. https://doi.org/10.1016/C2013-0-13663-X
12. Dean & Dalrymple (1991). *Water Wave Mechanics for Engineers and Scientists*. Advanced Series on Ocean Engineering: Volume 2. World Scientific Publishers, Toh Tuck Link, Singapore. https://doi.org/10.1142/1232
13. McCormick (2010). *Ocean Engineering Mechanics: With Applications*. Cambridge University Press, Cambridge, UK.

14. Amaechi C. V., Gillett N., Odijie A. C., Hou X., and Ye J. (2019). "Composite Risers for Deep Waters Using a Numerical Modelling Approach," *Compos. Struct.*, vol. 210, no. 2019, pp. 486–499, 2019. https://doi.org/10.1016/j.compstruct.2018.11.057
15. Amaechi, C.V. and Ye, J. (2021). Local tailored design of deep water composite risers subjected to burst, collapse and tension loads. Ocean Engineering 2021, https://doi.org/10.1016/j.oceaneng.2021.110196.
16. Amaechi, C.V. & Ye, J., (2017). A numerical modeling approach to composite risers for deep waters. In *International Conference on Composite Structures (ICCS20) Proceedings*, Paris, France; 4–7 September 2017; Società Editrice Esculapio: Bologna, Italy.
17. Amaechi C. V., Gillett N., Odijie A. C., Wang F., Hou X., and Ye J. (2019). "Local and Global Design of Composite Risers on Truss SPAR Platform in Deep waters," in *Proceedings of 5th International Conference on Mechanics of Composites*, Instituto Superior de Tecnico, Lisbon, Portugal, 1–4 July 2019; no. 20005, pp. 1–3.
18. Amaechi, C.V., Gillet N., Ye J. (2022). Tailoring the local design of deep water composite risers to minimise structural weight. *Journal of Composite Science.* 2022, 6, under review.
19. Sun, L, Zhang, X, Kang, Y, & Chai, S. "Motion Response Analysis of FPSO's CALM Buoy Offloading System." Proceedings of the ASME 2015 34th International Conference on Ocean, Offshore and Arctic Engineering. Volume 11: Prof. Robert F. Beck Honouring Symposium on Marine Hydrodynamics. St. John's, Newfoundland, Canada. May 31–June 5, 2015. V011T12A008. ASME. https://doi.org/10.1115/OMAE2015-41725
20. Amaechi, C.V. (2022). Novel design, hydrodynamics and mechanics of marine hoses in oil/gas applications. PhD Thesis. Lancaster University, Engineering Department, Lancaster, UK.
21. Kang, Y, Sun, L, Kang, Z, & Chai, S. "Coupled Analysis of FPSO and CALM Buoy Offloading System in West Africa." Proceedings of the ASME 2014 33rd International Conference on Ocean, Offshore and Arctic Engineering. Volume 8A: Ocean Engineering. San Francisco, California, USA. June 8–13, 2014. V08AT06A010. ASME. https://doi.org/10.1115/OMAE2014-23118
22. Qi, X., Chen, Y., Yuan, Q., Xu, G., and Huang K. 2017. CALM Buoy and Fluid Transfer System Study. In Proceedings of 27th *International Offshore and Polar Engineering Conference*. June 25–30, 2017. San Francisco, California, USA: ISOPE, pp. 932–939. Available at: https://onepetro.org/ISOPEIOPEC/proceedings-abstract/ISOPE17/All-ISOPE17/ISOPE-I-17-128/17225 (Accessed on 13th November, 2021).
23. Wang H., Ma G., Sun L., Hu K. (2017). Model test and coupled dynamic analysis of a deepwater FPSO with internal turret mooring system. *Brodogradnja* 68(4):42-55. DOI: 10.21278/brod68403
24. Gu, H., Chen, H.-C., and Zhao L. (2019). Coupled CFD-FEM simulation of hydrodynamic responses of a CALM buoy. *Ocean Systems Engineering,* Volume 9, Number 1, March 2019, pages 21-42. DOI: http://dx.doi.org/10.12989/ose.2019.9.1.021
25. Gu, H. (2016). Coupled mooring analysis of a CALM buoy by a CFD approach. Masters Thesis, Texas A&M University, Texas, USA.
26. Gu, H., Chen, H.-C., and Zhao L. (2017). "Coupled Mooring Analysis of a CALM Buoy by a CFD Approach." Paper presented at the 27th International Ocean and Polar Engineering Conference, San Francisco, California, USA, June 2017. Paper Number: ISOPE-I-17-223.
27. Amaechi, C.V., Chesterton C., Butler H.O., Gu Z., Odijie A.C., Wang F., Hou X., Ye J. (2022). Finite Element Model on the mechanical behaviour of Marine Bonded Composite Hose under internal pressure and external pressure. *J.Mar. Sci. Eng.*, accepted/in-print.

28. Amaechi C.V., Wang F., Ja'e I.A., Aboshio A., Odijie A.C., Ye J. (2022). A literature review on the technologies of bonded hoses for marine applications. *Ships and Offshore Structures*. 2022, https://doi.org/10.1080/17445302.2022.2027682.
29. Amaechi C.V., Chesterton C., Butler H.O., Wang F., Ye J. (2021). An Overview on Bonded Marine Hoses for sustainable fluid transfer and (un)loading operations via Floating Offshore Structures (FOS). *J. Mar. Sci. Eng*. 2021, 9(11):1236. https://doi.org/10.3390/jmse9111236.
30. Amaechi C.V., Chesterton C., Butler H.O., Wang F., Ye J. (2021). Review on the mechanics and design of marine bonded hoses for CALM buoys. *Ocean Engineering Journal*. 2021, **242,** https://doi.org/10.1016/j.oceaneng.2021.110062.
31. Amaechi, C.V., Wang, F.; Ye, J. Mathematical Modelling of Bonded Marine Hoses for Single Point Mooring (SPM) Systems, with Catenary Anchor Leg Mooring (CALM) Buoy Application—A Review. *J. Mar. Sci. Eng*. **2021**, *9*(11), 1179; **https://doi.org/10.3390/jmse9111179**.
32. Le Cunff, C. et al., 2007. Derivation of CALM Buoy coupled motion RAOs in Frequency Domain and Experimental Validation. In *International Society of Offshore and Polar Engineering Conference Proceedings*. Lisbon, Portugal: ISOPE, pp. 1–8.
33. Zhang S., Chen C., Zhang Q., Zhang D., Zhang F. (2015). Wave Loads Computation for Offshore Floating Hose Based on Partially Immersed Cylinder Model of Improved Morison Formula. The Open Petroleum Engineering Journal, 2015, 8, 130-137. Publisher Id TOPEJ-8-130, DOI: 10.2174/1874834101508010130
34. ABS, 2021. *Rules For Building And Classing - Single Point Moorings*, Texas, USA: American Bureau of Shipping. Available at: https://ww2.eagle.org/content/dam/eagle/rules-and-guides/current/offshore/8_rules-forbuildingandclassingsinglepointmoorings_2021/spm-rules-jan21.pdf (Accessed on 13th November, 2021).
35. API (2005). API RP 2SK - Design and analysis of stationkeeping systems for floating structures. 3rd edition, American Petroleum Institute (API), Texas, USA.
36. API (2017). API 17K -Specification for Bonded Flexible Pipe. ISO 13628-10 (Identical), Petroleum and natural gas industries-Design and operation of subsea production systems-Part 10: Specification for bonded flexible pipe. 3rd edition, American Petroleum Institute (API), Texas, USA.
37. OCIMF (2009). Guide to Manufacturing and Purchasing Hoses for Offshore Moorings (GMPHOM), Livingstone, UK: Witherby Seamanship International Ltd.
38. DNVGL, 2017. DNVGL-RP-F205 Global performance analysis of deepwater floating structures, Oslo, Norway: Det Norske Veritas & Germanischer Lloyd
39. DNVGL, 2016. DNVGL-OS-E403. Offshore laoding buoys. Oslo, Norway: Det Norske Veritas & Germanischer Lloyd. Available at: https://rules.dnv.com/docs/pdf/DNV/os/2015-07/DNVGL-OS-E403.pdf (Accessed on 13th November, 2021).
40. Bridgestone, J., 1976. *Study of causes of kinking in floating hoses at Petrobras/Tefran terminal. Report No. 6YMT-0011*, Japan.
41. Brown M.J. and Elliot L. (1987). A design tool for static underbuoy hose-systems. Applied Ocean Research, Vol.9, No. 3, Pages 171-180. https://doi.org/10.1016/0141-1187(87)90021-6
42. OCIMF (2020). A Study into Crane Loads Associated with Hose Handling at Offshore Terminals, OCIMF Info Paper, Version 6. Oil Companies International Marine Forum (OCIMF), London, UK. Available at: https://www.ocimf.org/media/58339/OC_INFOPAPER2961_CRANE_V6.pdf (Accessed on 14th February, 2021).

43. Liu B., Fu D., Zhang Y., Chen X. (2020). Experimental and numerical study on the wave force calculation of a partially immersed horizontal cylindrical float. International Journal of Naval Architecture and Ocean Engineering. Volume 12, 2020, Pages 733-742. https://doi.org/10.1016/j.ijnaoe.2020.08.002
44. Roveri, F.E., Volnei, Luís Sagrilo, S. & Cicilia, F.B., 2002. A Case Study on the Evaluation of Floating Hose Forces in a C.A.L.M. System. In *Internation Offshore and Polar Engineering Conference*. Kitakyushu, Japan,: ISOPE, pp. 190–197.
45. Ryu, S. et al., 2006. Prediction of Deepwater Oil Offloading Buoy Response and Experimental Validation. *International Journal of Offshore and Polar Engineering*, 16(3), pp.1–7.
46. Ricbourg, C. et al., 2006. Numerical and Experimental Investigations on Deepwater CALM Buoys Hydrodynamics Loads. In *Offshore Technology Conference Proceeding -OTC 18254 -PP*. Houston, Texas, USA: OnePetro, pp. 1–8.
47. Quash, J.E. & Burgess, S., 1979. Improving underbuoy hose system design using relaxed storm design criteria. In *Offshore Technology Conference Proceeding*. pp. 1827–1836.
48. Brady, I., Williams, S. & Golby, P., 1974. A study of the Forces Acting on Hoses at a Monobuoy Due to Environmental Conditions. In *Offshore Technology Conference Proceeding -OTC 2136*. Dallas, Texas, USA: OnePetro, pp. 1–10.
49. Saito, H. et al., 1980. Actual measurement of external forces on marine hoses for SPM. In *Offshore Technology Conference Proceeding -OTC 3803*. Houston, Texas, USA: OnePetro, pp. 89–97.
50. Young, R.A., Brogren, E.E. & Chakrabarti, S.K., 1980. Behavior Of Loading Hose Models In Laboratory Waves And Currents. In *Offshore Technology Conference Proceeding, OTC-3842-MS*. Houston, Texas, USA, pp. 421–428.
51. Amaechi, C.V., Wang F., Ye J. (2022). Investigation on hydrodynamic characteristics, wave-current interaction, and sensitivity analysis of submarine hoses attached to a CALM buoy. *J. Mar. Sci. Eng.*, 2022; 10(1):120. https://doi.org/10.3390/jmse10010120.
52. Duggal, A. & Ryu, S., 2005. The dynamics of deepwater offloading buoys. In Singapore, ed. *WIT Transactions on The Built Environment*. Paper FSI05026FU, WIT Press. Available at: https://www.witpress.com/Secure/elibrary/papers/FSI05/FSI05026FU.pdf
53. O'Donoghue, T. & Halliwell, A.R., 1990. Vertical bending moments and axial forces in a floating marine hose-string. *Engineering Structures*, 12(4), pp.124–133. DOI: 10.1016/0141-0296(90)90018-n
54. O'Donoghue T., Halliwell A.R. (1988). Floating Hose-Strings Attached To A Calm Buoy. Offshore Technology Conference, Houston, Texas, May 1988. Paper Number: OTC-5717-MS https://doi.org/10.4043/5717-MS
55. Ziccardi, J.J. & Robins H.J. (1970). Selection of the hose systems for SPM tanker terminals. Paper presented at the Offshore Technology Conference (OTC), Houston, Texas, USA. Paper Number: OTC-1152-MS, 2nd Annual Offshore Technology Conference, Houston, April 21–23, 1970. https://doi.org/10.4043/1152-MS
56. Amaechi, C.V.; Wang, F.; Ye, J. (2021). Understanding the fluid-structure interaction from wave diffraction forces on CALM buoys: Numerical and analytical solutions. *Ships and Offshore Structures.* 2021, DOI: 10.1080/17445302.2021.2005361.
57. Amaechi, C.V., Wang, F.; Ye, J. (2022). Numerical studies on CALM buoy motion responses, and the effect of buoy geometry cum skirt dimensions with its hydrodynamic waves-current interactions. *Ocean*

Eng., 244 (7), 110378. https://doi.org/10.1016/j.oceaneng.2021.110378.

58. Kang, Z., Zhang, C., Ni, W., and Xu, X. (2017). Research on Hydrodynamic Calculation Method of Deepwater CALM Buoy. In *International Ocean and Polar Engineering*. San Francisco, California, USA: ISOPE, pp. 217–224.
59. Edward C., Kr. Dev D.A. (2021) Assessment of CALM Buoys Motion Response and Dominant OPB/IPB Inducing Parameters on Fatigue Failure of Offshore Mooring Chains. In: Okada T., Suzuki K., Kawamura Y. (eds) Practical Design of Ships and Other Floating Structures. PRADS 2019. Lecture Notes in Civil Engineering, vol 64. Springer, Singapore. https://doi.org/10.1007/978-981-15-4672-3_35
60. Wang, D. & Sun, S., 2014. An Analytical Solution of Wave Exciting Loads on CALM Buoy with Skirt. *Applied Mechanics and Materials*, 478, pp.254–258.
61. Cozijn, J.L. & Bunnik, T.H.J., 2004. Coupled Mooring Analysis for a Deep water CALM Buoy; OMAE2004-51370. In *International Conference on Offshore Mechanics and Arctic Engineering (OMAE) Proceedings*. Vancouver, British Columbia, Canada: ASME, pp. 1–11.
62. Cozijn, H., Uittenbogaard, R. & Brake, E. Ter, 2005. Heave , Roll and Pitch Damping of a Deepwater CALM Buoy with a Skirt. In *International Society of Offshore and Polar Engineering Conference Proceedings*. Seoul, Korea: ISOPE, pp. 388–395.
63. Woodburn, P, Gallagher, P, Naciri, M, & Borleteau, J. "Coupled CFD Simulation of the Response of a Calm Buoy in Waves." Proceedings of the ASME 2005 24th International Conference on Offshore Mechanics and Arctic Engineering. 24th International Conference on Offshore Mechanics and Arctic Engineering: Volume 3. Halkidiki, Greece. June 12–17, 2005. pp. 793-803. ASME. https://doi.org/10.1115/OMAE2005-67063
64. Amaechi, C.V., Wang F., Ye J. (2022). An investigation on the vortex effect of a CALM buoy under water waves using Computational Fluid Dynamics (CFD). Inventions 2021, under review.
65. Monroy C., Ducrozet G., Bonnefoy F., Babarit A., Gentaz L., Ferrant P. (2011). RANS Simulations of a Calm Buoy in Regular and Irregular Seas using the SWENSE Method. International Journal of Offshore and Polar Engineering (IJOPE), The International Society of Offshore and Polar Engineers 2011, 21(4), pp.264-271. hal-01145146. Available at: https://hal.archives-ouvertes.fr/hal-01145146/document (Accessed on 13th November, 2021).
66. Abbaszadeh M., Dehghan M., Khodadadian A., Heitzinger C. (2019). Analysis and application of the interpolating element free Galerkin (IEFG) method to simulate the prevention of groundwater contamination with application in fluid flow. Journal of Computational and Applied Mathematics 368(155):112453 https://doi.org/10.1016/j.cam.2019.112453
67. Parvizi M., Khodadadian A., Eslahchi M.R. (2020). Analysis of Ciarlet–Raviart mixed finite element methods for solving damped Boussinesq equation. Journal of Computational and Applied Mathematics, Volume 379, 1 December 2020, 112818 https://doi.org/10.1016/j.bios.2019.111527
68. Abbaszadeh M., Dehghan M., Khodadadian A., Noii N., Heitzinger C., Wick T. (2021). A reduced-order variational multiscale interpolating element free Galerkin technique based on proper orthogonal decomposition for solving Navier–Stokes equations coupled with a heat transfer equation: Nonstationary incompressible Boussinesq equations. Journal of Computational Physics, Volume 426, 1 February 2021, 109875 https://doi.org/10.1016/j.jcp.2020.109875
69. Bluewater, 2011. *Bluewater Turret Buoy- Technical Description*, Amsterdam, The Netherlands: Bluewater Energy Services. Available at: https://www.bluewater.com/wp-content/uploads/2013/04/digitale-

brochure-TurretBouy-Tech-description.pdf. (Accessed on 13th November, 2021).

70. EDesign (2016). Edinburgh Designs Ltd., Edinburgh, UK. Available at: http://www4.edesign.co.uk/product/wave-generating-software/ (Accessed on 26th September, 2021).
71. Zhang, D., Aggidis, G., Wang, Y., Gu, X., Li, W., Chen, Y. (2015) Wave tank experiments on the power capture of a multi-axis wave energy converter. *Journal of Marine Science and Technology*, 20 (3). pp. 520-529. https://doi.org/10.1007/s00773-015-0306-5
72. Zhang D.H., Aggidis G.A., Wang Y.F., Andy M., Li W. (2013) Experimental results from wave tank trials of a multi-axis wave energy converter. Appl Phys Lett 103(103901):1–4 https://doi.org/10.1063/1.4820435
73. Doyle, S., & Aggidis, G.A. (2021). Experimental investigation and performance comparison of a 1 single OWC, array and M-OWC. Renewable Energy, 168, 365-374. https://doi.org/10.1016/j.renene.2020.12.032
74. MARINET (2015). D2 27 Manual of wave instrumentation survey of laboratories. WP2: Marine Energy System Testing - Standardisation and Best Practice. MARINET (Marine Renewables Infrastrcuture Network for emerging Energy Technologies). Available at: https://www.marinet2.eu/wp-content/uploads/2017/04/D2.27-Manual-of-Wave-Instrumentation-1.pdf (Accessed on 13th November, 2021).
75. Imetrum, (2017). Digital Image Correlation in Video Gauge™. Available at: https://www.imetrum.com/documents/product-sheets/digital-image-correlation.pdf (Accessed on 24th April, 2021).
76. Imetrum 2016. Video Gauge User Manual: Version 5.4.0. Imetrum Limited, Bristol, UK. pp. 1-153.
77. Milad, M., Green, S., Ye, J., (2018). Mechanical properties of reinforced composite materials under uni-axial and planar tension loading regimes measured using a non-contact optical method, Composite Structures, Vol. 202, pp. 1145-1154. DOI: https://doi.org/10.1016/j.compstruct.2018.05.070
78. Aboshio A, Green S, Ye J. (2015). Experimental investigation of the mechanical properties of neoprene coated nylon woven reinforced composites. Composite Structures, Volume 120, February 2015, Pages 386-393 https://doi.org/10.1016/j.compstruct.2014.10.015
79. Odijie, A.C., 2016. Design of paired column semisubmersible hull. PhD Thesis. Lancaster University, Lancaster, UK. Available at: https://doi.org/10.17635/lancaster/thesis/39 (Accessed on 24th April, 2021).
80. NI (2003). LabView: Getting Started with LabView. National Instruments Manual, Part Number 323427A-01. National Instruments, North Mopac Expressway Austin, Texas, U.S.A. Available at: https://www.ni.com/pdf/manuals/323427a.pdf (Accessed on 6th January, 2022).
81. NI (2013). LabView: Getting Started with LabView. National Instruments Manual, Part Number 373427J-01. National Instruments, North Mopac Expressway Austin, Texas, U.S.A. Available at: https://www.ni.com/pdf/manuals/373427j.pdf (Accessed on 6th January, 2022).
82. WIT (2019). WIT Motion User Manual. WIT Motion (Xingji Jia Yuan), Shenzhen City, Guangdong Province, China. Available at: hhttps://wiki.wit-motion.com/english (Accessed on 26th September, 2021).
83. WitMotion (2020). Wit Motion Bluetooth Sensor. WIT Motion (Xingji Jia Yuan), Shenzhen City, Guangdong Province, China. Available at: http://www.wit-motion.com/english.php (Accessed on 26th September, 2021).
84. Samsung (2017). Samsung Galaxy S8 | S8+ Smartphone User Manual. Samsung Electronics America Inc., New Jersey, USA. Available at: http://files.customersaas.com/files/Samsung_G950U_Galaxy_S8_User_Manual.pdf or https://galaxys8manualguide.com/ (Accessed on 26th September, 2021).

85. Samsung (2021). Samsung Galaxy S8- Support, Warranty Information, Solutions & Tips. Samsung Electronics America Inc., New Jersey, USA. Available at: https://www.samsung.com/uk/support/model/SM-G950FZVABTU/ (Accessed on 26th September, 2021).
86. AKASO (2020). AKASO Action Camera EK7000 User Manual. Akaso Tech, USA. Available at: https://www.akasotech.com/usermanual/detail?category=1&product=11&name=EK7000 or https://www.akasotech.com/usermanual/brave4.pdf (Accessed on 26th September, 2021).
87. Amaechi, C.V., Wang, F.; Ye, J. (2021). Numerical Assessment on the Dynamic Behaviour of Submarine Hoses Attached to CALM Buoy Configured as Lazy-S under Water Waves. *J. Mar. Sci. Eng.* **2021**, *9*(10), 1130; **https://doi.org/10.3390/jmse9101130**
88. Amaechi, C.V., Wang F., Hou X., and Ye J. (2019). Strength of submarine hoses in Chinese-lantern configuration from hydrodynamic loads on CALM buoy. *Ocean Engineering, vol. 171, no. 2019, pp. 429–442, 2019. https://doi.org/10.1016/j.oceaneng.2018.11.010*.
89. Amaechi C. V., Ye J., Hou X., and Wang F.-C. (2019), "Sensitivity Studies on Offshore Submarine Hoses on CALM Buoy with Comparisons for Chinese-Lantern and Lazy-S Configuration OMAE2019-96755," in *38th International Conference on Ocean, Offshore and Arctic Engineering, Glasgow, Scotland, June 9–14, 2019*.
90. Orcina, 2014. *OrcaFlex Manual, Version 9.8a*, Ulverton, Cumbria, UK: Orcina Ltd.
91. Orcina, 2022. *OrcaFlex Manual, Version 11.0f* [electronic online version of manual and documentation), Ulverton, Cumbria, UK: Orcina Ltd.. Available at: https://www.orcina.com/SoftwareProducts/OrcaFlex/Documentation/index.php (Accessed on 4th January, 2022)
92. Orcina, 2021. *Orcaflex Documentation, Version 11.0f.* Available at: https://www.orcina.com/webhelp/OrcaFlex/Default.htm (Accessed on 24th April, 2021).
93. Wang, F., Chen J., Gao S., Tang K., Meng X. (2017). Development and sea trial of real-time offshore pipeline installation monitoring system. *Ocean Engineering*, 146, pp.468–476. https://doi.org/10.1016/j.oceaneng.2017.09.016.
94. Tracker (2016). Tracker Video Analysis and Modeling Tool- Tracker home page. Available at: https://physlets.org/tracker/ (Accessed on 4th January, 2022)
95. Tracker (2016). Tracker Video Analysis and Modeling Tool- Tracker 6.0.2. Available at: http://www.opensourcephysics.org/items/detail.cfm?ID=7365 (Accessed on 4th January, 2022).
96. Douglas Brown, Robert Hanson, and Wolfgang Christian (2016). Tracker Video Analysis and Modeling Tool. O.S.P- Open Source Physics. Available at: ComPADRhttps://www.compadre.org/osp/items/detail.cfm?ID=7365 (Accessed on 4th January, 2022).